Design of a Ventilated Façade Integrating a Luminescent Solar Concentrator Photovoltaic Panel

Supplementary Materials

Giulio Mangherini [1,*], Paolo Bernardoni [2,*], Eleonora Baccega [3], Alfredo Andreoli [1], Valentina Diolaiti [1] and Donato Vincenzi [1,4]

[1] Department of Physics and Earth Sciences, University of Ferrara, 44122 Ferrara, FE, Italy; donato.vincenzi@unife.it (D.V.)
[2] Department of Chemical, Pharmaceutical and Agricultural Sciences, University of Ferrara, 44121 Ferrara, FE, Italy
[3] Department of Architecture, University of Ferrara, 44121 Ferrara, FE, Italy
[4] Consorzio Futuro in Ricerca, 44122 Ferrara, FE, Italy
* Correspondence: giulio.mangherini@unife.it (G.M.); paolo.bernardoni@unife.it (P.B.); Tel.: +39-0532-974270 (G.M.)

The temperature measured by the thermistors were acquired by using a modular system composed by several electronic boards. This system was developed in the Photovoltaic Laboratory of the University of Ferrara, it is called Multi_IO and it was able to acquire both digital and analog input and output.

A block diagram summarizing the components of the acquisition system is presented in Figure S1:

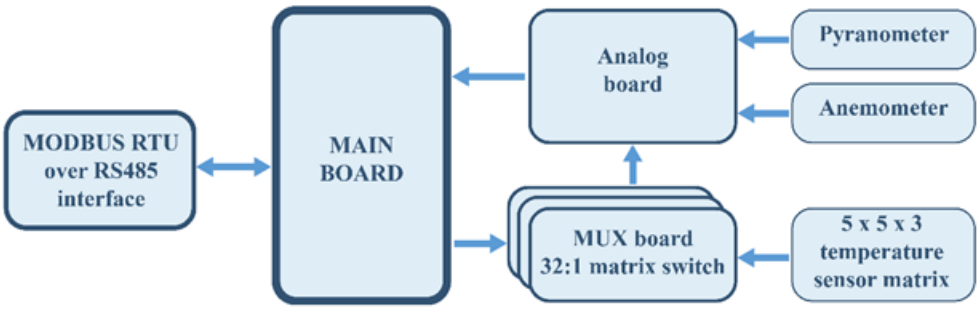


Figure S1 Block diagram presenting the components and the logical connection of the data acquisition system.

The physical connection to the Main board of the Multi_IO system occurred through an unshielded twisted pair (UTP) cable with RJ45 connectors. The data was transmitted to a data acquisition software developed in LabView using as physical layer the serial RS485 and the standard MODBUS RTU protocol to manage the communication. The UTP cable allows also to power the Main board and all the daughter boards without the necessity of an additional power supply. The first addon board was an analog expansion board called Multi_IO_Analog, used both to digitalize the analog signals from the sensors network, and to acquire the meteorological data. In particular, the Global Normal Irradiance (GNI) with respect to the LSC panel main surface was collected by using a Delta OHM pyranometer, LP PYRA 03, directly to the Multi_IO_Analog board. The wind parameters were measured by a Davis Instruments anemometer, DW 6410, connected to both the Main board, which registered the velocity, and to the the Multi_IO_Analog board for the wind direction logging. The temperature measured by the NTC sensors were acquired thanks to three additional expansion boards called Multi_IO_MUX, each of which was

dedicated to one of the three 5x5 sub matrixes that crossed all the façade layers. Indeed, the Multi_IO_MUX configuration allowed to independently connect each NTCs to an input of the Multi_IO_Analog board.

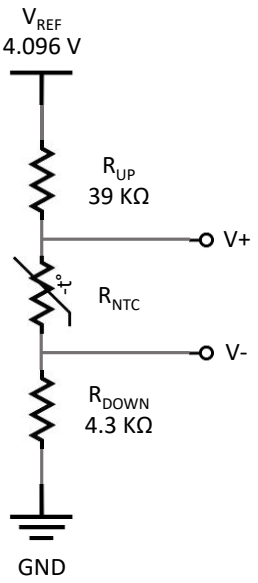


Figure S2. Schematic of the voltage divider used to constrain the voltage drop on the NTC between 0 and 2.048V corresponding to temperatures ranging from +∞ to -8.6 °C. The purpose of the pull-down resistor is to avoid the voltage swing limit of the input amplifier.

Negative Temperature Coefficient (NTC) thermistors are sensors whose resistance decreases as temperature increases, following a particular case of the Steinhart–Hart equation that can be expressed by Equation (S1):

$$R_{NTC} = R_0 \cdot e^{B\left(\frac{1}{T}-\frac{1}{T_0}\right)}, \quad \text{(S1)}$$

where B is a characteristic coefficient, which for the NTCs used in this research is equal to 3435 K. R_0 is 10 KΩ and corresponded to the NTC resistance at temperature $T_0 = 298\ K$.

The signal given by each NTC was collected thanks to a voltage divider with three resistors, in which the NTC was the central variable resistor (see Figure S2). This configuration allowed a proper bias of the analog signal digitalized by the Multi_IO_Analog board and ensured the measurements of voltage difference between the thermistor edges (V+ and V-) with an error introduced by the acquisition electronics one order of magnitude smaller (1‰) than the NTC intrinsic one (1%). The value of the pull-up, R_{UP}, and pull-down resistor, R_{DOWN}, guaranteed a proper operation range for the analog-to-digital conversion of the Multi_IO_Analog board. The board has four 16bit sigma-delta differential analog-to-digital converters (ADCs) with a reference voltage of 2.048 V (1‰), and the presence of R_{UP} allows to use the full input range of the ADCs in the -8 °C to 70 °C temperature range. On the other hand, the purpose of R_{DOWN} is to avoid having a signal too close to the V- rail of the ADCs input amplifiers.

In Figure S3 the range of measurable temperature as a function of the differential voltage across the thermistor is presented.

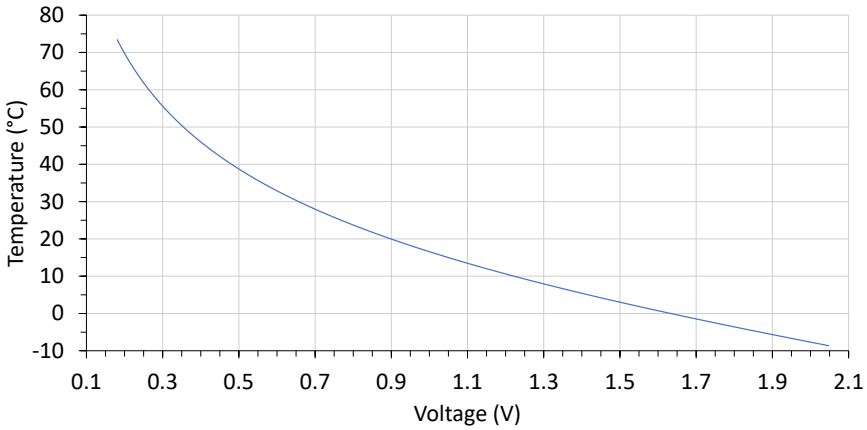


Figure S3 Measurable temperature range by the NTC sensors as a function the potential difference between V+ and V-.

A detailed presentation of the Multi_IO electrical components and of the data acquisition software was omitted as they were not essential for the interpretation of the results presented within this work, and it will be presented in a further contribution.

In Figure S4 (a) the Characteristic I-V and P-V curves of the LSC panel are presented. The curves were acquired on the 04th May 2021 at noon with an illumination (GNI) of 480W/m². Figure S3 (b) shows the efficiency and the power produced by the module between the 04th and 09th May 2021.

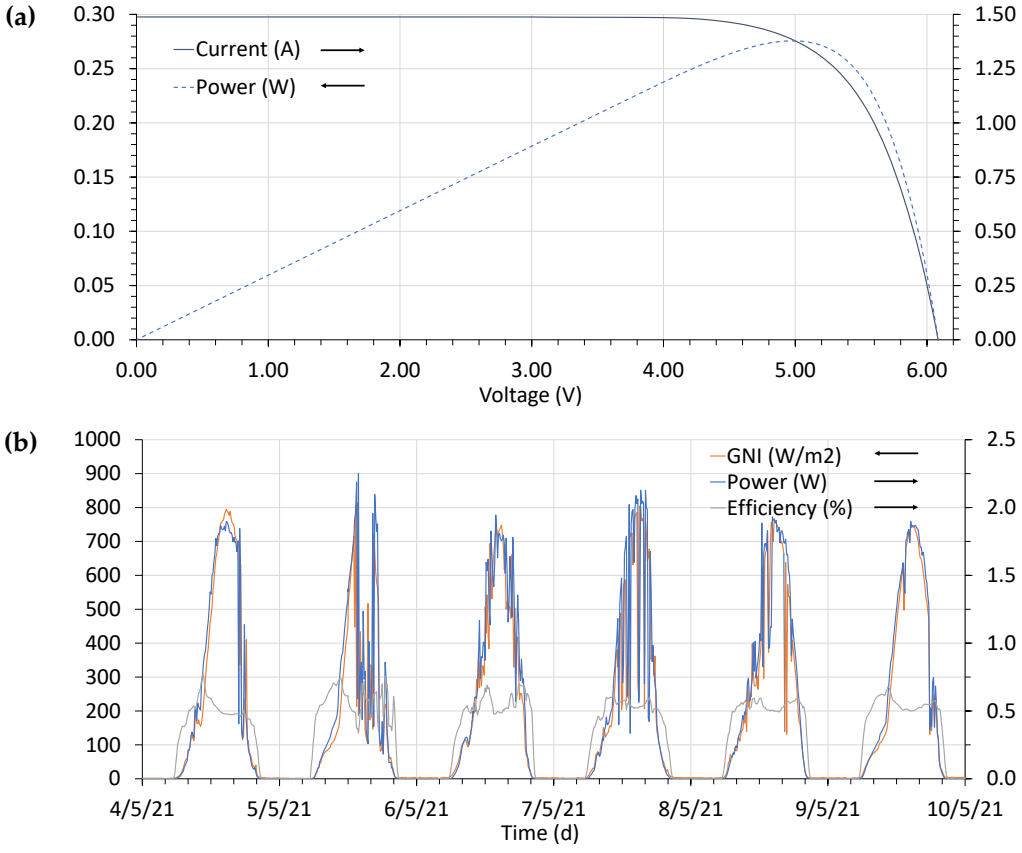


Figure S4 (a) LSC panel I-V and P-V curves measured under a GNI of 480W/m² (04th May 2021). (b) Efficiency and power produced by the module between the 4th and 9th May 2021.

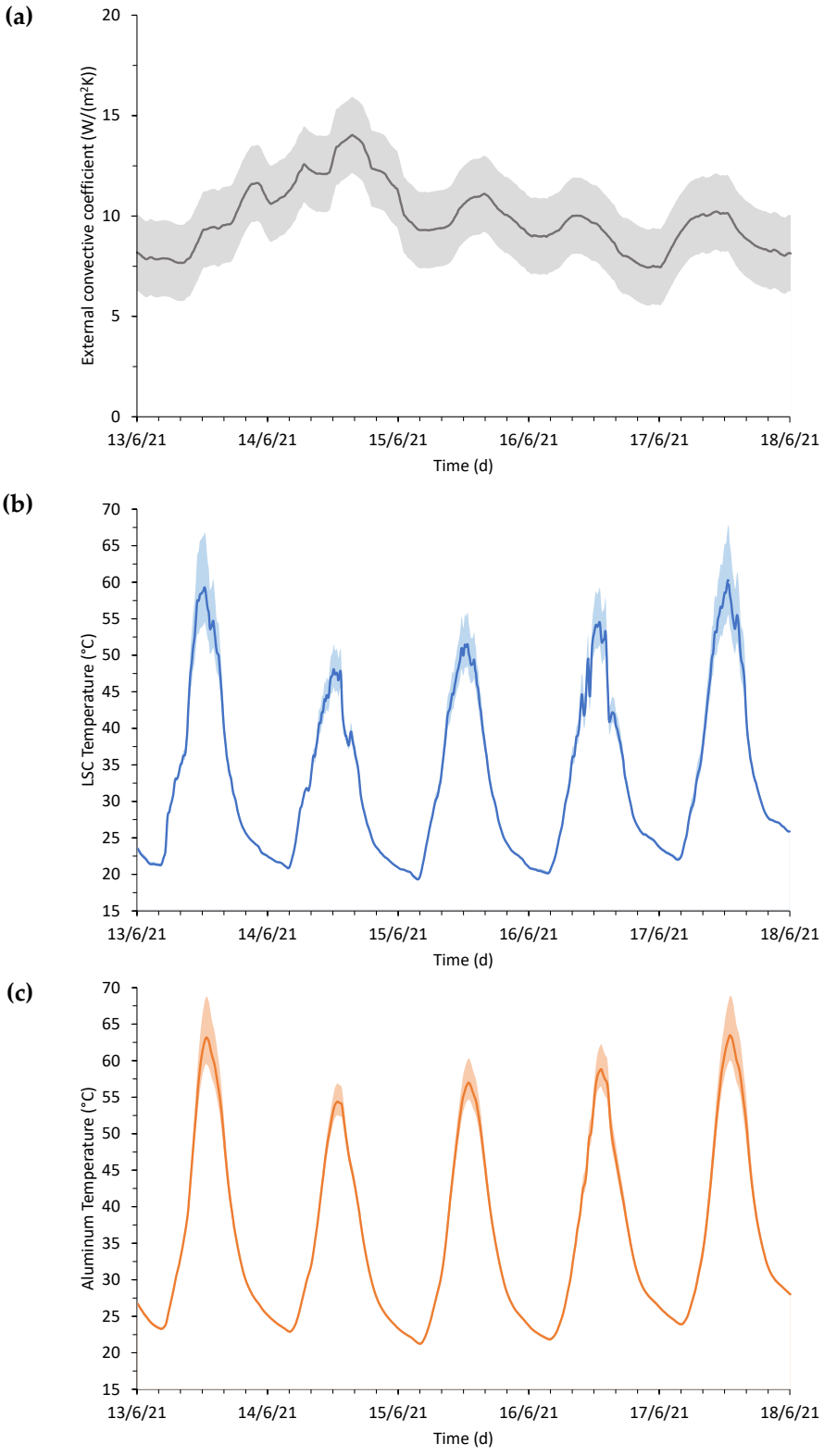
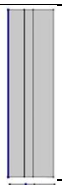
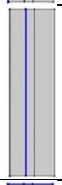
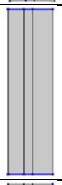
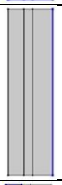
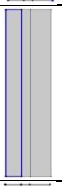
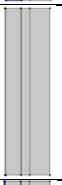
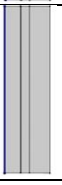


Figure S5. (a) Range of possible convective heat flux according to the anemometer accuracy. Simulated (b) LSC, and (c) Al pane temperature ranges according to the different h used in the CFM.

Figure S5 (a) displays the range spanned by the possible wind convective coefficient due to the anemometer accuracy (shaded area), and the solid line highlights the h value used in the simulations. A variation of h in the COMSOL models affects both the LSC and the Al temperature, the range of possible LSC and Al temperatures according to the wind convection coefficient inserted in the simulation is presented in Figure S5 (b) and (c) (shaded intervals). This comparison highlights the considerable impact of h variation on

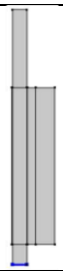
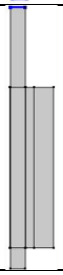
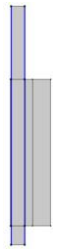
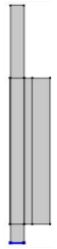
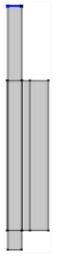
the temperature on the LSC and Al temperature, thus leading to the decision to use the third NTC sensor of the central section for the validation and calibration procedures. The solid lines in Figure S5 (b) and (c) underline the temperature values compared with the experimental data. Considering the complexity of the boundary conditions inserted in both the Closed Façade Model (CFM) and in the Open Façade Model (OFM) they were summarized using Table S1 and S2.

Table S1 Summary of the boundary conditions inserted in the CFM.

FEM Model	Physics	Boundary condition	COMSOL Layout
Closed Façade Model	HT[1]	Convective heat flux: $T_{ext} = T_{amb}$	
		Thermal contact: $R_{EQ} = 2$ (K·m²)/W	
		Insulated boundaries	
		Measured temperature: Layer 1	
	SPF	Wall: no-slip condition	
		Pressure point constrain: Atmospheric pressure	
	RAD[1]	Measured GNI	

[1] These boundary conditions were imposed also in the OFM, except for the top and bottom thermal insulation of the air channel.

Table S2 Summary of the new boundary conditions inserted in the OFM.

FEM Model	Physics	Boundary condition	COMSOL Layout
Open Façade Model[2]	HT	Inflow: $T_{ext} = T_{amb}$ +2 °C	
		Outflow	
		Wall: no-slip condition	
	SPF	Inlet: v = 0 m/s	
		Outlet: Atmospheric pressure	

[2] Only the differences with respect to the Closed Façade Model have been reported.